

UDC 661.937:544.022.38:546.083:544.015.3:544.43

DOI: 10.15372/CSD20180515

## Effect of Process Parameters of the Phase Inversion Method on the Morphology of Microtubular Membranes

N. V. NIFTALIYEVA<sup>1,2</sup>, E. V. SHUBNIKOVA<sup>1</sup>, and A. P. NEMUDRY<sup>1</sup><sup>1</sup>*Institute of Solid State Chemistry and Mechanochemistry, Siberian Branch, Russian Academy of Sciences, Novosibirsk, Russia*

E-mail: niftalievanaatalya@gmail.com

<sup>2</sup>*Novosibirsk State University, Novosibirsk, Russia*

### Abstract

The effects of a series of process parameters (the composition of external coagulant and the air-gap distance) on the morphology of oxygen-permeable microtubular (MT) membranes were explored. The latter were prepared from non-stoichiometric  $\text{Ba}_{0.5}\text{Sr}_{0.5}\text{Co}_{0.8-x}\text{Mo}_x\text{Fe}_{0.2}\text{O}_{3-\delta}$  perovskites (BSCFM $x$ ). It was demonstrated by scanning electron microscopy that the specific porous structure of MT membranes vanished when increasing the air gap between the draw hole and the bath with coagulant to 15 cm or using an ethanol solution. The oxygen permeability of MT membranes based on  $\text{Ba}_{0.5}\text{Sr}_{0.5}\text{Co}_{0.8-x}\text{Mo}_x\text{Fe}_{0.2}\text{O}_{3-\delta}$  ( $x = 0, 0.02, 0.05, 0.10$ ) with the optimum morphology in air and under  $\text{CO}_2$  was examined.

**Key words:** ceramic microtubular membranes, oxygen-permeable membranes, non-stoichiometric oxides, oxygen permeability

### INTRODUCTION

Non-stoichiometric oxides with the perovskite structure have mixed oxygen-electronic conductivity and may be regarded as promising membranes in chemical, gas, and energy industries. Among other things, they may be used to produce synthesis gas ( $\text{CO} + \text{H}_2$ ) in catalytic membrane reactors. Oxygen-permeable membranes are generally divided into planar and tubular. Currently, the planar geometry of membranes is very common, as it ensures high heat and mass transfer, has a compact assembly and is prepared by standard ceramic methods. In turn, the tubular geometry prevails over planar one in hermetization processes. Nevertheless, both types have a significant drawback, such as substantial temperature gradients along the membrane leading to material decomposition during thermal cycling. In order to address this challenge, microtubular

(MT) membranes are suggested to be used. They favourably differ not only by higher oxygen flows due to small thickness of the gas-tight layer located between the porous layers but also by improved mechanical strength [1–3]. Furthermore, MT membranes have elevated thermal strength and simplicity upon hermetization and scaling.

One of the most promising ways of preparation of MT membranes is the phase inversion method. According to the data of [4–6], control over the microstructure of the resulting membranes may be carried out by varying process parameters of the procedure. For example, that may be achieved by varying precipitation time, paste and coagulant temperatures, the air-gap distance [7], a pair of solvent and coagulant, etc.

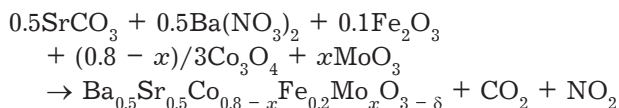
According to papers [1, 2], non-stoichiometric oxides based on perovskites with the formula  $\text{Ba}_{0.5}\text{Sr}_{0.5}\text{Co}_{0.8-x}\text{Fe}_{0.2}\text{Mo}_x\text{O}_{3-\delta}$  (BSCFM $x$ ) have high chemical and thermal stability, hence, they may

be regarded as membrane materials for separation processes of oxygen from air.

The objective of this research work was to produce MT membranes based on non-stoichiometric BSCFM $x$  oxides and also to explore the effect of process parameters of the gas inversion method on the morphology and transport characteristics of oxygen-permeable MT membranes.

## EXPERIMENTAL

The investigated non-stoichiometric oxides with the formula  $\text{Ba}_{0.5}\text{Sr}_{0.5}\text{Co}_{0.8-x}\text{MoFe}_{0.2}\text{O}_{3-\delta}$  (BSCFM $x$ ) ( $0 \leq x \leq 0.10$ ) were synthesised by the ceramic method. Chemically pure metal oxides, nitrates, and carbonates were starting materials used in synthesis. The formation reaction for BSCFM $x$  is as follows:



The phase composition and structure of the samples were determined using Bruker D8 Advance X-ray diffractometer ( $\text{CuK}_\alpha$  radiation) with a Lynx-Eye liner detector. The structure refinement of oxides with the formula BSCFM $x$  was carried out by full-profile Rietveld analysis using the Topas 4.2 software (Bruker, Germany).

Microtubular membranes were produced by phase inversion. The paste was prepared by mixing a powder of a mixture of oxides after heating the solvent (N-methyl-2-pyrrolidone, NMP) and the polymer (polysulphone) in a 12 : 4 : 1 ratio, respectively, at 900 °C. For the purposes of complete homogenization, the resulting mixture was mixed in a PROSTAR PR6000 roll mill in steel drums with one grinding body over 40 h. The paste viscosity controlled with a Fungilab Smart rotary viscometer was equal to 67 Pa · s.

The morphology of MT membranes was investigated by scanning electron microscopy (SEM) using the HitachiTM 1000 electron microscope with an accelerating voltage of 15 kV and Swift-ED-TMEDX X-ray spectrum analyser. High-temperature research on the oxygen permeability of MT membranes was carried out using the purposely designed reactor [2]. The optical heating of the membrane ( $l \sim 8$  cm,  $d \sim 0.4$  cm) to the operating temperature was performed by alternating current transmission therethrough [3]. Gas flows were generated using a UFPGS-4 gas mixer (SoLO, Novosibirsk). The gas flow at the membrane exit was analysed using the QMS 200

quadrupole mass spectrometer. Measuring the stability of oxygen flows through MT membranes under  $\text{CO}_2$  was carried out at a given partial pressure of oxygen from the feed side of the membrane ( $p\text{O}_{2,1} = 0.2$  atm) and at a  $\text{CO}_2$  concentration of 10 % in a mixture with He (a flow rate of 90 mL/min).

## RESULTS AND DISCUSSION

Figure 1 presents X-ray diffraction patterns of the synthesised  $\text{Ba}_{0.5}\text{Sr}_{0.5}\text{Co}_{0.8-x}\text{Fe}_{0.2}\text{Mo}_x\text{O}_{3-\delta}$  compounds (BSCFM $x$ ) ( $x = 0, 0.02, 0.05, 0.10$ ) obtained by slow cooling in air. According to the data of X-ray phase analysis (XPA), monophasic products with the cubic perovskite structure are formed upon the synthesis of BSCFM $x$  oxides ( $x = 0, 0.02, 0.05$ ).

The space group of symmetry is  $Pm\bar{3}m$ . Apart from the main cubic perovskite reflexes, the X-ray diffraction pattern of the BSCFM $x$  sample ( $x = 0.10$ ) has additional ones that are referred to the phase of double  $\text{Ba}/\text{SrCoMoO}_6$  perovskite with the tetragonal  $I4/m$  structure. The findings are in agreement with the results of the paper [2].

### Variation of the air-gap distance

According to the data of [9], one may control the microstructure and morphology of MT membranes by varying process parameters of the phase inversion process. We investigated the air-gap distance between the draw hole and the bath with the coagulant, and also the composition of

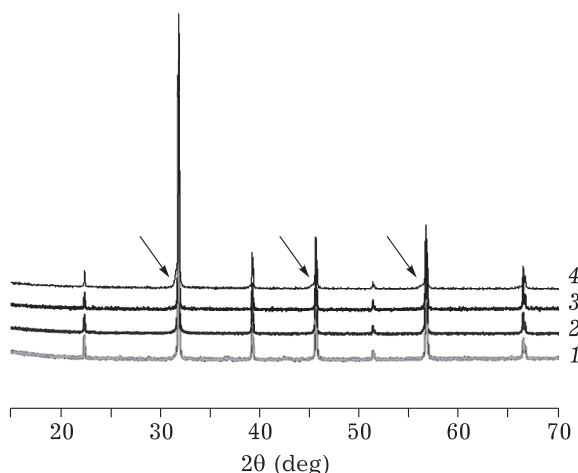


Fig. 1. X-ray diffraction patterns of samples with the formula  $\text{Ba}_{0.5}\text{Sr}_{0.5}\text{Co}_{0.8-x}\text{Fe}_{0.2}\text{Mo}_x\text{O}_{3-\delta}$  (BSCFM $x$ )  $x$ : 0 (1), 0.02 (2), 0.05 (3), 0.10 (4). Arrows indicate the double perovskite phase.

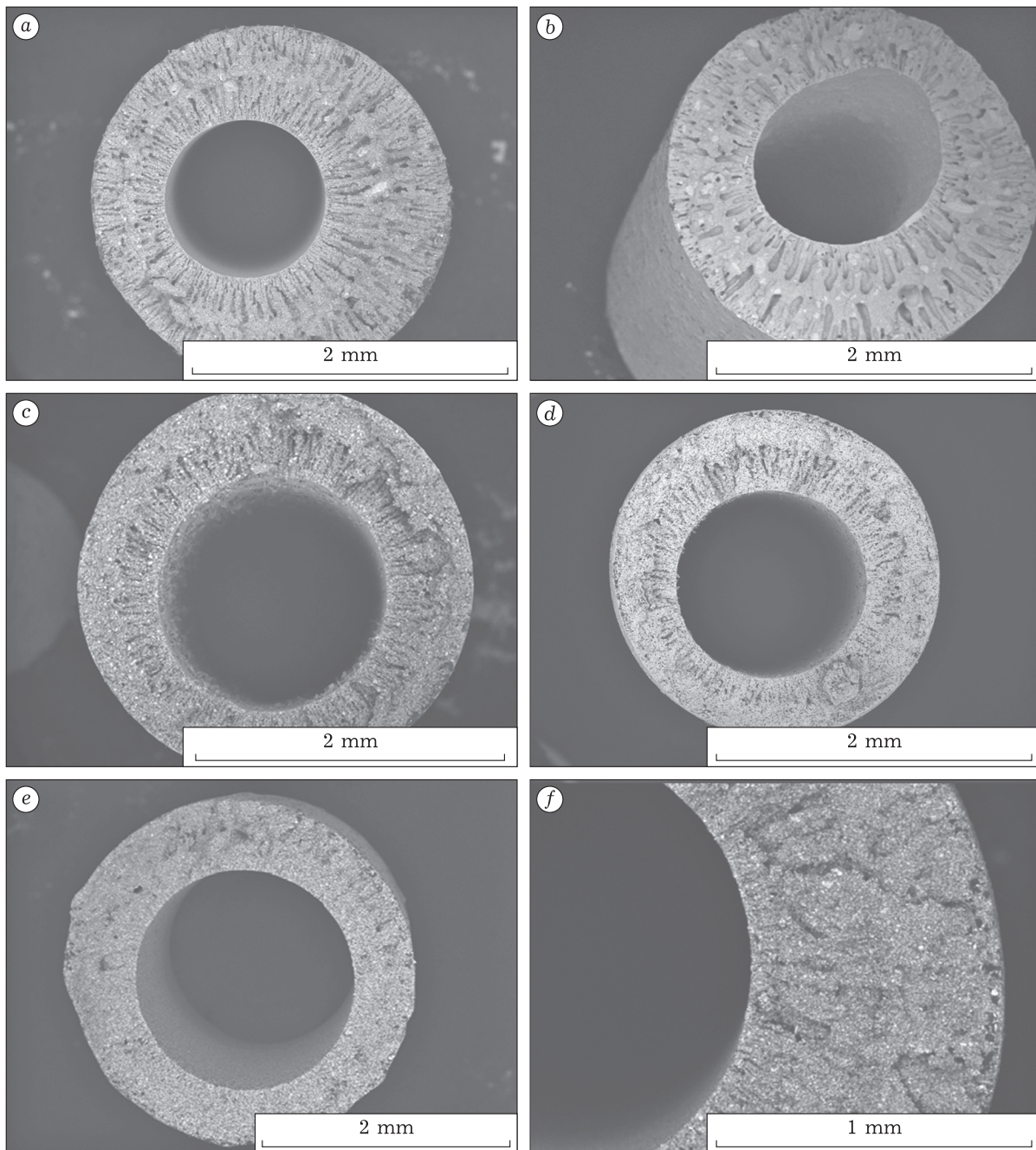


Fig. 2. Micrographs of MT membranes composed of BSCFM2 ( $T_{\text{sin}} = 1150\text{ }^{\circ}\text{C}$ ) before (a, c, and e) and after sintering (b, d, and f). Air-gap distance (cm): 0.5 (a, b), 5 (c, d), 15 (e, g).

external coagulant on the microstructure of the resulting MT membranes.

Analysis of the microstructure of the resulting MT membranes based on  $\text{Ba}_{0.5}\text{Sr}_{0.5}\text{Co}_{0.78}\text{Fe}_{0.2}\text{Mo}_{0.02}\text{O}_{3-\delta}$  (BSCFM2) was carried out using SEM. As can be seen from micrographs of MT membranes with the formula BSCFM2 before (Fig. 2, a, c, and e) and after sintering (see Fig. 2, b, d, and g) at a temperature of  $1150\text{ }^{\circ}\text{C}$ , the microstructure of MT membranes is preserved hereupon. When the minimum

air-gap distance is 0.5 cm, 230–245  $\mu\text{m}$  elongated pores are formed as channels from the external and internal sides of the membrane (finger-like in English-language literature) with sizes of and a 20–50  $\mu\text{m}$  thin gas-tight layer between them (see Fig. 2, a and b). When the air-gap distance is increased to 5 cm, the external layer disappears and the membrane is comprised of the external gas-tight and internal porous layers with thicknesses of 180–200 and 230–250  $\mu\text{m}$ , respectively

(see Fig. 2, *c* and *d*). There are no open pores in the membrane when the air gap is 15 cm (see Fig. 2, *e*). Microtubular membrane walls become gas-tight upon sintering (see Fig. 2, *g*).

The disappearance of the external porous layer is related to a local increase in the viscosity at the external side of the membrane due to solvent evaporation and moisture condensation from the air [8].

Thus, it is possible to obtain ceramic MT membranes with different positions and thicknesses of the gas-tight layer by changing the value of the air gap. In turn, this may fundamentally affect both oxygen permeability processes and product mechanical strength. According to the data of [10], MT membranes with a thin gas-tight layer located between layers with open porosity have the maximum values of oxygen flows.

#### *Variation of the composition of external coagulant*

External coagulant composition also has an effect on the microstructure of MT membranes obtained by phase inversion [8]. In this work, water and an aqueous solution of ethanol with a mass fraction of 30 and 50 % were used. As can be seen from micrographs of the resulting MT mem-

branes based on BSCFM2 (an air gap of 0.5 cm and a sintering temperature of 1150 °C), when water is used as external coagulant, elongated (finger-like) pores are formed as channels from the outer and inner sides of the membrane, separated by a gas-tight layer (Fig. 3, *a*). When a 30 % ethanol solution is used as external coagulant (see Fig. 3, *b*), pores at the external side of the membrane disappear, whereas at internal one they are decreased in size. If a 50 % solution of ethanol is used, open porosity (finger-like) of the MT membrane disappears and the membrane becomes gas-tight when sintering.

According to literature data, the effect of ethanol solutions with different concentrations on pore formation is due to the mass transfer between the solvent and the coagulant. Table 1 gives diffusion coefficients for NMP solvent and ethanol [11].

According to [11], the suspension precipitation process may be tentatively divided into two types. One of them is slow liquid-solid phase separation, in which a relatively small amount of coagulant diffuses into a suspension (paste). Another type assumes quick phase separation, in which a large amount of coagulant quickly diffuses into the

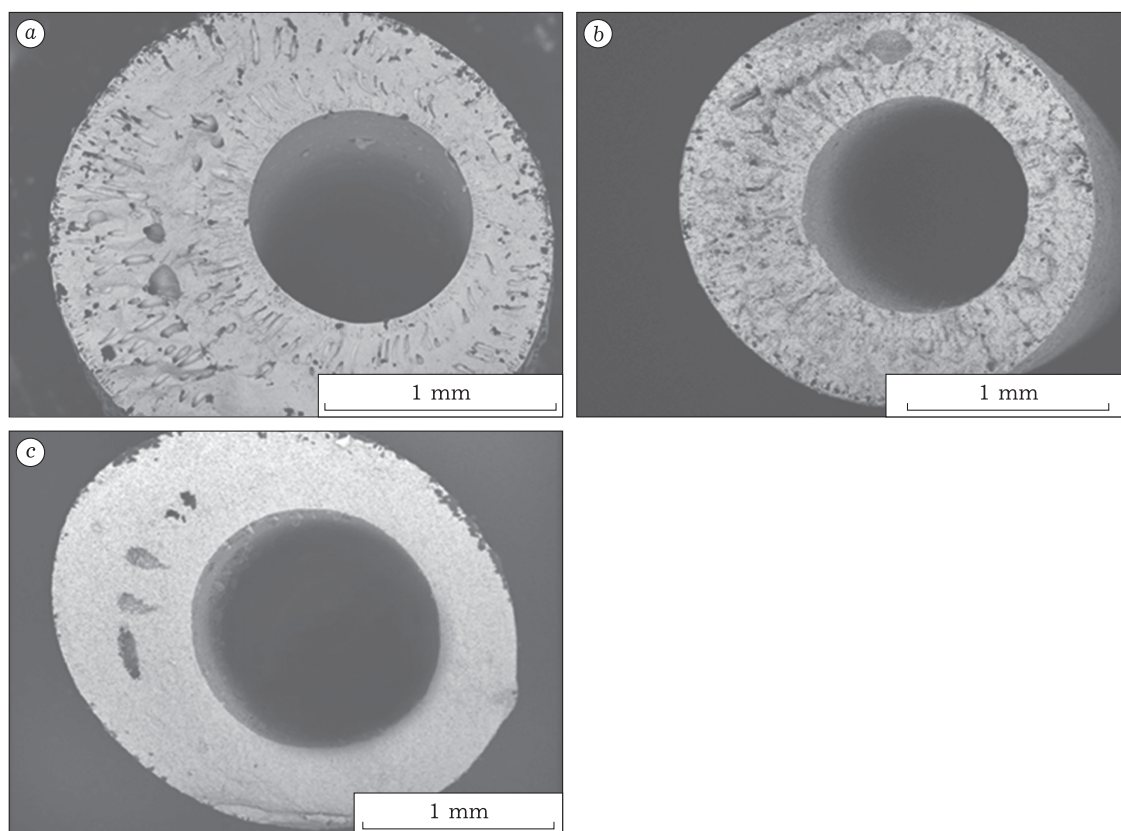


Fig. 3. Micrographs of MT membranes composed of BSCFM2. The species were produced by phase inversion with variation of the composition of external coagulant: *a* – water; *b*, *c* – aqueous ethanol solution with a mass fraction of 30 % (*b*) and 50 % (*c*).

TABLE 1

Diffusion coefficients of NMP and ethanol ( $D$ ) [11]

Compound/medium	$D \cdot 10^{-6}$ , $\text{cm}^2/\text{s}$
NMP/water	8.04
NMP/ethanol	8.51
Water/NMP	14.80
Ethanol/NMP	10.76

suspension. As it follows from the comparison of  $D_{\text{water/NMP}}$  and  $D_{\text{ethanol/NMP}}$  diffusion coefficients, the use of water as a coagulant is likely to facilitate quick phase separation, unlike ethanol solutions. As a result, there are fast coagulation and the formation of elongated pores as channels after suspension contact with water. When ethanol solutions are used, solid phase precipitation is held back by the relatively slow diffusion of coagulant into a paste. In this case, polymer concentration is locally increased due to complete solvent removal and an insufficient amount of coagulant diffusing into suspension, which facilitates suspension coagulation and the formation of an initially non-porous layer. The latter would hinder the formation of elongated pores, which confirms the resulting experimental data (see Fig. 3, b and c).

Optimum process parameters were determined when making MT membranes for SOFC cathode materials by phase inversion. The former induce the developed microstructure of materials and include the use of water as an external coagulant, an air-gap distance of 0.5 cm.

#### Stability research on of MT membranes under $\text{CO}_2$

One of the main standards that are imposed on SOFC cathode materials is the stability of the latter in the atmosphere that contains hydrocarbon oxidation products, such as  $\text{CO}$ ,  $\text{CO}_2$ , and  $\text{H}_2$ . This research has examined the stability of MT membranes based on non-stoichiometric oxides with the formula  $\text{Ba}_{0.5}\text{Sr}_{0.5}\text{Co}_{0.8-x}\text{Fe}_{0.2}\text{Mo}_x\text{O}_{3-\delta}$  (BSCF),  $\text{Ba}_{0.5}\text{Sr}_{0.5}\text{Co}_{0.78}\text{Fe}_{0.2}\text{Mo}_{0.02}\text{O}_{3-\delta}$  (BSCFM2),  $\text{Ba}_{0.5}\text{Sr}_{0.5}\text{Co}_{0.75}\text{Fe}_{0.2}\text{Mo}_{0.05}\text{O}_{3-\delta}$  (BSCFM5), and  $\text{Ba}_{0.5}\text{Sr}_{0.5}\text{Co}_{0.7}\text{Fe}_{0.2}\text{Mo}_{0.1}\text{O}_{3-\delta}$  (BSCFM10) under  $\text{CO}_2$ .

According to [12], non-stoichiometric BSCF oxide is chemically unstable under  $\text{CO}_2$  due to the formation of  $\text{SrCO}_3$  and  $\text{BaCO}_3$  on the surface [13]. Nevertheless, introducing  $\text{Mo}^{6+}$  cations makes it possible to prevent material splitting and stabilize oxygen flows due to the following factors: 1) the formation of a composite material consisting of double perovskite phase and cubic perovskite [2];

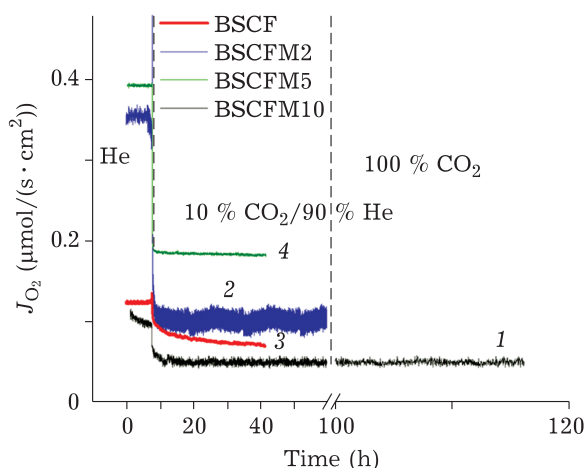


Fig. 4. Oxygen flows of MT membranes on BSCFM $x$  ( $x = 0, 0.02, 0.05, 0.10$ ) under  $\text{CO}_2$  at  $T = 630^\circ\text{C}$  vs time. Conditions are as follows:  $J_{\text{He}} = 90 \text{ mL/min}$ ;  $p_{\text{O}_{2.1}} = 0.2 \text{ atm}$ .

2) a decrease in oxide basicity when acidic molybdenum cations are introduced.

Figure 4 presents oxygen flows through MT membranes composed of BSCFM $x$  ( $x = 0, 0.02, 0.05, 0.10$ ) in the atmosphere with 10%  $\text{CO}_2$  content at  $630^\circ\text{C}$  vs time. Oxygen flows remain stable and do not undergo splitting over 70 and 110 h for BSCFM2 and BSCFM10, respectively.

#### CONCLUSION

We have produced MT membranes based on  $\text{Ba}_{0.5}\text{Sr}_{0.5}\text{Co}_{0.8-x}\text{Fe}_{0.2}\text{Mo}_x\text{O}_{3-\delta}$  oxides, BSCFM $x$  ( $x = 0, 0.02, 0.05, 0.10$ ), by phase inversion. Variation in the morphology of  $\text{Ba}_{0.5}\text{Sr}_{0.5}\text{Co}_{0.8-x}\text{Fe}_{0.2}\text{Mo}_x\text{O}_{3-\delta}$  MT membranes, BSCFM $x$  ( $x = 0.02$ ), has been demonstrated using scanning electron microscopy when varying the air-gap distance and the composition of external coagulant. The optimum process parameters of the preparation process of MT membranes for SOFC cathode materials *via* this method have been determined. They are as follows: an air-gap distance of 0.5 cm and the use of water as an external coagulant. According to oxygen permeability research, MT membranes composed of BSCFM $x$  ( $x = 0.02, 0.05, 0.10$ ) are stable under  $\text{CO}_2$ .

#### Acknowledgements

The work was accomplished under financial support of the state task of the Institute of Solid State Chemistry and Mechanochemistry SB RAS (project 0301-2019-0002).

## REFERENCES

- 1 Markov A. A., Savinskaya O. A., Patrakeev M. V., Nemudry A. P., Leonidov I. A., Pavlyukhin Yu. T., Ishchenko A. V., Kozhevnikov V. L., *J. Solid State Chem.* 2009. Vol. 182. P. 799–806.
- 2 Shubnikova E. V., Bragina O. A., Nemudry A. P., *J. Ind. Eng. Chem.* 2018. Vol. 59. P. 242–250.
- 3 Popov M. P., Bychkov S. F., Nemudry A. P., *Solid State Ionics.* 2017. Vol. 312. P. 73–79.
- 4 Kim H. J., Tyagi R. K., Fouda A. E., Jonasson K., *J. Appl. Polym. Sci.* 1996. Vol. 62. P. 621–629.
- 5 Zheng Q. Z., Wang P., Yang Y. N., Cui D. J., *J. Membr. Sci.* 2006. Vol. 286. P. 711.
- 6 Amirilargani M., Saljoughi E., Mohammadi T., Moghbeli M. R., *Polym. Eng. Sci.* 2010. Vol. 50. P. 885–893.
- 7 Kingsbury B. F. K., Li K., *J. Membr. Sci.* 2009. Vol. 328. P. 134–140.
- 8 Cong Ren. Fabrication and Characterization of Anode Supported Micro-Tubular Solide Oxide Fuel Cell by Phase Inversion Method [Electronic resource]: PhD thesis. University of South Carolina, Columbia, 2015. 128 p. URL: <https://scholarcommons.sc.edu/etd/3134/> (date of application 25.07.2018).
- 9 Sumi H., Yamaguchi T., Hamamoto K., Suzuki T., Fujishiro Y., *J. Am. Ceram. Soc.* 2013. Vol. 96. P. 3584–3588.
- 10 Tan X., Liu N., Meng B., Liu S., *J. Membr. Sci.* 2011. Vol. 378. P. 308–318.
- 11 Reuvers A. J., Smolders C. A., *J. Membr. Sci.* 1987. Vol. 34. P. 6786.
- 12 Yan A. Y., Bin L., Dong Y. L., Tian Z. J., Wang D. Z., Cheng M. J., *Appl. Catal.,B.* 2008. Vol. 80. P. 24–31.
- 13 Arnold M., Wang H. H., Feldhoff A., *J. Membr. Sci.* 2007. Vol. 293. P. 44–52.